Available online at www.sciencedirect.com

SciVerse ScienceDirect

Nuclear Physics B (Proc. Suppl.) 235–236 (2013) 49–54

NUCLEAR PHYSICS B PROCEEDINGS SUPPLEMENTS

www.elsevier.com/locate/npbps

Super-Kamiokande's Solar ν Results

Michael Smy[a] for the Super-Kamiokande Collaboration

[a] *Department of Physics & Astronomy, 3117 Frederick Reines Hall, UC Irvine, CA 92697-4575, USA*

Abstract

Super-Kamiokande observed 57,700 recoil electrons from solar ^{8}B and hep neutrino-electron scattering between 3.489 and 19.489 MeV kinetic energy in 3,904 live days. The interaction rate is 45.1±0.7% of the rate expected from a pure ν_e ^{8}B flux of $5.25\times10^6/\mathrm{cm}^2\mathrm{s}$ (and a hep flux of $7.88\times10^3/\mathrm{cm}^2\mathrm{s}$). The observed recoil electron spectrum favors a flat suppression over distortions predicted by standard neutrino flavour oscillation parameters by 1.1 to 1.9σ. The observed day/night variation of -2.8±1.1(stat)±0.5(syst)% is consistent with zero at the 2.3σ level. The oscillation analysis of this data determines the solar neutrino mass^2 splitting $\Delta m^2_{21} = 4.69^{+1.80}_{-0.83}\times10^{-5}\mathrm{eV}^2$, consistent within 1.5 to 2σ with KamLAND's anti-neutrino measurement.

Keywords: Solar Neutrinos, Flavor Oscillations

1. Introduction

Since the upgrade of its electronics in August 2008, Super-Kamiokande (SK), a 50,000 ton water Cherenkov detector viewed by 11,000 (inner detector: 32 kton) and 1,900 (outer detector: 18kton) photomultiplier tubes (PMTs), collected 1069 live days of solar ^{8}B (and hep) neutrino data using elastic scattering on electrons. There are four phases of the experiment: SK-I (11,000 PMTs) ran for about 5 years until an accident destroyed 2/3 of the PMTs. The surviving 5,000 PMTs were re-distributed for SK-II. In SK-III and IV the original PMT configuration is restored. Super-Kamiokande detected 57,700 solar neutrino interactions in 3,904 live days (combining all four phases). Any results which include SK-IV data are very preliminary.

2. Super-Kamiokande Solar ν Interaction Rate

In [1] we reported an improvement of the systematic uncertainty of the absolute interaction rate in SK-III which allowed us to determine this rate more precisely than SK-I [2], even though the exposure was much less. Due to a mistake in the calculation of the expected interaction rate, the extracted flux (assuming all solar ν's to be ν_e) was incorrect: it should have been $2.39\times10^6/(\mathrm{cm}^2\cdot\mathrm{sec})$ instead of $2.32\times10^6/(\mathrm{cm}^2\cdot\mathrm{sec})$. The impact of this mistake on SK-III's spectral and day/night measurements is negligible. The solar neutrino interaction rate measurement of the fourth phase is so far the most accurate, since the exposure is almost as large as the first phase, and the systematic uncertainty is as small as the third phase. Combining all phases, the interaction rate is 45.1±0.7% of the rate expected from a pure ν_e ^{8}B flux of $5.25\times10^6/\mathrm{cm}^2\mathrm{s}$ (and a hep flux of $7.88\times10^3/\mathrm{cm}^2\mathrm{s}$). The interaction rates of all phases are consistent with each other within their statistical uncertainty.

3. Reconstruction of Multiple Coulomb Scattering

In this conference, we present a new analysis method for the lower energy bins of the recoil electron spectrum. We reconstruct the amount of multiple Coulomb scattering of electrons using the PMT hit pattern of the Cherenkov cone. Lower energy electron hit patterns (e.g. from radioactive backgrounds such as

0920-5632/$ – see front matter
http://dx.doi.org/10.1016/j.nuclphysbps.2013.03.010

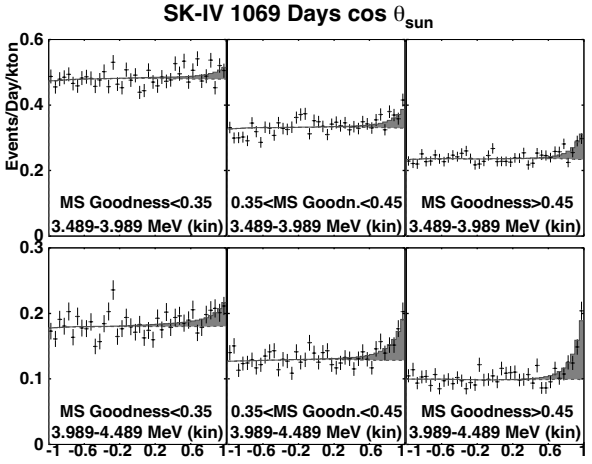

Fig. 1. Angular distribution of solar neutrino-electron elastic scattering candidates in the lowest two recoil electron energy bins. Each energy bin is divided into three bins by reconstructed multiple Coulomb scattering (left=large, middle=medium, right=small). The shaded region shows the solar neutrino component of the fit.

^{214}Bi) are more isotropic than those of the higher energy solar neutrino recoil electrons. This hit pattern anisotropy is measured by a "direction fit goodness": we construct a list of event direction candidate vectors from all possible PMT hit pairs (each pair contributing two). We sum up those direction candidates, which are consistent with each other (within about 50 degrees). The length of the sum vector (normalized by twice the number of hit pairs) is a measure of the scattering the particle undergoes as it emits Cherenkov light. The solar neutrino candidates of a particular recoil electron energy bin are then grouped in three sub-samples of "multiple scattering goodness" (MS goodness). All three angular distributions with respect to the solar direction (cos θ_{sun}) are fit simultaneously to a signal and a background component. We require the ratios of the three signal components to agree with solar neutrino Monte Carlo, but the three background components remain unconstrained and independent. Figure 1 shows the measured cos θ_{sun} distributions (as well as the fits) of the lowest two recoil electron energy bins. There is less background at higher MS goodness, and the solar ν elastic scattering peak sharpens. This analysis method improves the statistical uncertainty of the number of signal events by about 10%. The additional systematic uncertainty is small (Table 1 and 2 list it for SK-III and SK-IV) compared to the statistical uncertainty. We use this new method for recoil energies below 7.489 MeV (kinetic energy). We observe a significant signal at a (kinetic) recoil electron energy threshold as low as 3.489 MeV.

4. Recoil Electron Spectrum

To search for spectral distortions (due to neutrino flavour oscillations) of the recoil electron spectrum, we divide the data into recoil electron energy bins and form the ratio of the measured event rate divided by the calculated event rate (based on a pure ν_e ^{8}B flux of 5.25×10^6/cm^{2}s, and a hep flux of 7.88×10^3/cm^{2}s). Figure 2 shows this spectral distortion for each phase of the experiment as well as energy-correlated systematic uncertainties. Tables 1 and 2 list the energy-uncorrelated systematic uncertainties of SK-III and SK-IV. The systematic uncertainties of the total rate as well as the lower recoil electron energy bins are much smaller in SK-IV. Figure 3 plots the spectral distortions of a fit of the ^{8}B and hep fluxes to all SK solar data using four different spectral predictions. For illustration, Figure 3 also shows a statistical average of these four spectra, but the fit is to the separate spectra of Figure 2. Two of the four fits assume standard oscillation parameters determined by a combined fit to

E_{kin}/MeV	3.5-4	4-4.5	4.5-5	5-5.5	5.5-6
trig. eff	-	2.4%	2.4%	0.9%	0.1%
recon. gdn	-	2.0%	2.0%	1.8%	1.5%
hit pattern	-	-	-	-	-
hit cluster	-	2.0%	2.0%	2.0%	2.0%
external	-	0.1%	0.1%	0.1%	0.1%
vertex fit	-	0.5%	0.5%	0.1%	0.1%
bkg shape	-	0.8%	0.2%	0.8%	0.2%
signal fit	-	2.1%	2.1%	0.7%	0.7%
cross sctn	-	0.2%	0.2%	0.2%	0.2%
MS gdn.	-	0.3%	0.3%	0.3%	1.7%
total	**-**	**4.4%**	**4.2%**	**3.0%**	**3.1%**
E_{kin}/MeV	6-6.5	6.5-7	7-7.5	7.5-20	4-20
trig. eff	-	-	-	-	0.5%
ang. reso.	-	-	-	-	0.7%
recon. gdn	1.3%	1.0%	0.1%	0.1%	0.4%
hit pattern	0.3%	0.3%	0.3%	0.3%	0.3%
hit cluster	-	-	-	-	0.5%
external	0.1%	0.1%	0.1%	0.1%	0.3%
vertex fit	0.1%	0.1%	0.1%	0.1%	0.5%
2nd vtx fit	-	-	-	-	0.5%
spallation	-	-	-	-	0.2%
bkg shape	0.2%	0.2%	0.2%	0.2%	0.1%
signal fit	0.7%	0.7%	0.7%	0.7%	0.7%
cross sctn	0.2%	0.2%	0.2%	0.2%	0.5%
MS gdn.	1.7%	1.7%	1.7%	-	0.4%
total	**2.3%**	**2.1%**	**1.9%**	**0.8%**	**1.4%**

Table 1: Energy-uncorrelated systematic uncertainties of the SK-III spectrum and rate. Figure 2 plots the energy-correlated systematic uncertainties .The column «4-20» refers to the total rate uncertainty.

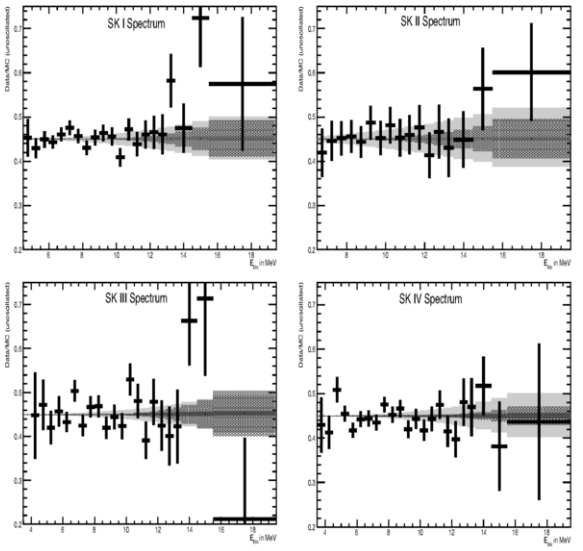

Fig. 2. Spectral distortion of SK-I (upper left), SK-II (upper right), SK-III (bottom left), and SK-IV (bottom right). The shaded light (dark) gray area is the ±1σ systematic uncertainty of the energy scale (neutrino spectrum), the dotted area is the ±1σ systematic uncertainty of the energy resolution. Energy-uncorrelated uncertainties for SK-III and IV are shown in Table 1 and 2.

E_{kin}/MeV	3.5-4	4-4.5	4.5-5	5-5.5	5.5-6
trig. eff	4.5%	0.4%	-	-	-
recon.gdn	0.8%	0.8%	0.8%	0.8%	0.6%
hit pattern	-	-	-	-	-
hit cluster	1.1%	0.6%	0.4%	-	-
external	0.1%	0.1%	0.1%	0.1%	0.1%
vertex fit	0.5%	0.5%	0.3%	0.1%	0.1%
bkg shape	2.9%	1.0%	0.8%	0.2%	0.1%
signal fit	2.1%	2.1%	2.1%	0.7%	0.7%
cross sctn	0.2%	0.2%	0.2%	0.2%	0.2%
MS gdn.	0.4%	0.3%	0.3%	0.3%	1.7%
total	**6.0%**	**2.6%**	**2.5%**	**1.2%**	**2.0%**
E_{kin}/MeV	6-6.5	6.5-7	7-7.5	7.5-20	3.5-20
trig. eff	-	-	-	-	0.1%
ang. reso.	-	-	-	-	0.4%
recon.gdn	0.6%	0.6%	0.1%	0.1%	0.3%
hit pattern	0.6%	0.6%	0.3%	0.3%	0.3%
hit cluster	-	-	-	-	0.3%
external	0.1%	0.1%	0.1%	0.1%	0.2%
vertex fit	0.1%	0.1%	0.1%	0.1%	0.2%
spallation	-	-	-	-	0.4%
bkg shape	0.1%	0.1%	0.1%	0.1%	0.1%
signal fit	0.7%	0.7%	0.7%	0.7%	0.7%
cross sctn	0.2%	0.2%	0.2%	0.2%	0.5%
MS gdn.	1.7%	1.7%	1.7%	-	0.4%
total	**2.1%**	**2.1%**	**1.9%**	**0.8%**	**1.1%**

Table 2: Energy-uncorrelated systematic uncertainties of the SK-IV spectrum and rate. Figure 2 plots the energy-correlated systematic uncertainties. The column «3.5-20» lists the total rate uncertainty.

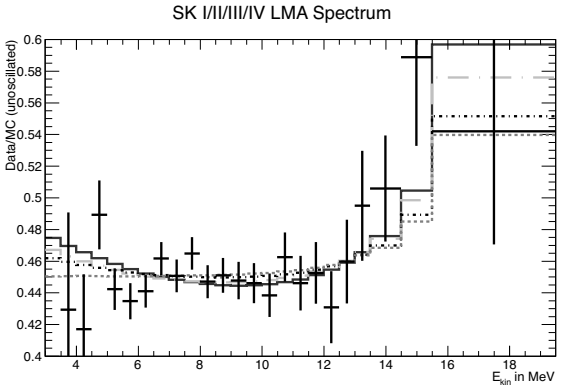

Fig. 3. Statistical average of SK-I, II, III and IV Spectral Distortion (error bars). Overlaid are LMA predictions at the KamLAND (solid dark gray) and solar (light gray dash dotted) Δm^2 as well as assuming a 31.7% ν_e flavour content independent of energy (dark gray dash dotted) and energy-independent flavour and cross section ratio (gray dotted).

oscillation parameters	χ^2	φ_{8B}/ (cm^2·sec)	φ_{hep}/ (cm^2·sec)
$\sin^2\theta_{12}$=0.304 , Δm^2=7.41·10^{-5}eV^2	SK spec: 76.90 (global: 82.55)	5.42·10^6 (5.32·10^6)	39.4·10^3 (8.05·10^3)
$\sin^2\theta_{12}$=0.314 , Δm^2=4.84·10^{-5}eV^2	SK spec: 74.59 (global: 79.33)	5.42·10^6 (5.32·10^6)	35.7·10^3 (8.05·10^3)
flat probability	SK spec: 73.60	(5.51·10^6)	(35.4·10^3)
flat prob., dσ ratio	SK spec: 73.26	(5.49·10^6)	(31.8·10^3)

Table 3: χ^2 of the spectrum fits of Figures 2 and 3. We assume $\sin^2\theta_{13}$=0.025.

all solar ν data (with or without KamLAND reactor antineutrino data [3]). A third case assumes an energy-independent ν_e flavour content of 31.7%. In addition to that, the fourth fit also requires an energy-independent differential cross section ratio $d\sigma_{\mu/\tau}(E_\nu,E_e)/d\sigma_e(E_\nu,E_e)$ of 16%. Table 3 gives the χ^2 for each combined fit. SK favors a flat suppression over the distortions of the standard oscillation parameters by 1.1 to 1.9σ (based on the observed $\Delta\chi^2$). Constraining the hep neutrino flux to $(7.88\pm1.26)\times10^3/(cm^2sec)$ slightly increases the χ^2 differences, but does not change the conclusions qualitatively. Non-standard interactions could explain the absence of spectral distortion in the considered energy region [4], however at present we cannot rule out the standard oscillation scenario.

5. Day/Night Effect

The matter density of the Earth affects solar neutrino flavour oscillations while the sun is below the horizon. For most oscillation parameters, this "day/night effect" leads to an enhancement of the ν_e flavour content. The most straight-forward search for this effect is to separately measure the interaction rates

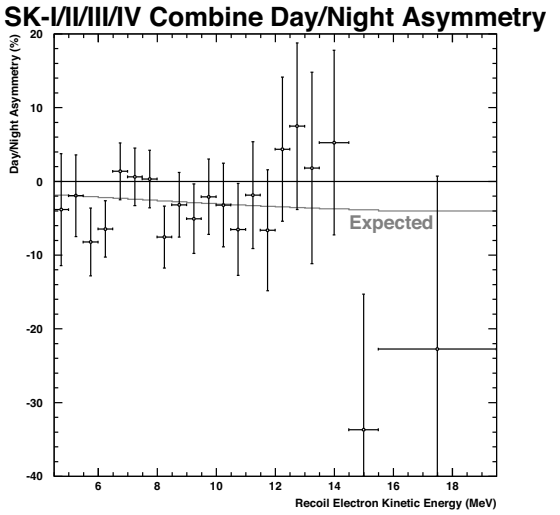

Fig. 4. Energy dependence of the fitted day/night amplitude for $\Delta m^2=4.84\cdot10^{-5}eV^2$ (and $\sin^2\theta_{12}=0.304$).

during the day φ_D and the night φ_N and form the asymmetry $A_{DN}= (\varphi_D-\varphi_N)/(0.5(\varphi_D+\varphi_N))$. A more sophisticated method [5] performs a maximum likelihood fit of the amplitude of the expected variation to the entire data sample; the amplitude is then expressed as an asymmetry to allow direct comparison with the simple method. Because the amplitude fits depend on the assumed shape of the day/night variation (given for each energy bin in [5]), they necessarily depend on the oscillation parameters as well. Figure 4 shows the amplitude fit as a function of recoil electron energy for $\Delta m^2=4.84\cdot10^{-5}eV^2$ and $\sin^2\theta_{12}=0.304$. Table 3 summarizes the amplitude fit of each phase (same oscillation parameters). It also lists the day/night asymmetries of each phase as well as the combined value. As there is no good way of combining the day/night asymmetries from different SK phases (or different experiments), Table 3 just gives a simple statistical average. The measured day/night amplitude differs from zero by 2.3σ. Figure 5 displays the combined amplitude fit as a function of the

experiment	D/N amplitude	A_{DN}
SK-I	-2.0±1.7±1.0%	-2.1±2.0±1.3%
SK-II	-4.3±3.8±1.0%	-6.3±4.2±3.7%
SK-III	-4.3±2.7±0.7%	-5.9±3.4±1.3%
SK-IV	-2.8±1.9±0.7%	-5.2±2.3±1.4%
SK I/II/III/IV	**-2.8±1.1±0.5%**	-4.0±1.3±0.8%

Table 4: Day/Night Amplitude and Asymmetry for each SK-Phase. The middle column assumes $\Delta m^2=4.84\cdot10^{-5}eV^2$ (and $\sin^2\theta_{12}=0.304$). The combined value of the right column is a simple statistical average, while the middle column combined value takes energy threshold and resolution into account.

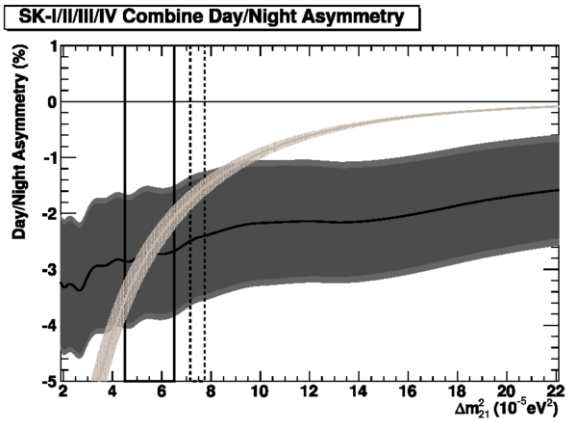

Fig. 5. Dependence of the amplitude fit on Δm^2 (statistical error: dark gray band; stat.+syst. error: lighter gray band). Overlaid is the expected amplitude (light gray band) as well as the allowed range from solar experiments (solid rectangle) and from KamLAND (dashed rectangle).

solar Δm^2. Superimposed are the expected amplitude and the allowed range in Δm^2 from the combined solar neutrino data fit and from KamLAND [3].

The SNO experiment searched for day/night variation of the charged-current interaction rate on deuterium [6]. It defines a day/night asymmetry of the electron-neutrino survival probability and models that asymmetry with the function $a_0+a_1(E_\nu-10MeV)/MeV$. SNO measures $a_0=-0.046\pm0.034$ and $a_1=0.016\pm0.027$. Using $\Delta m^2=4.84\cdot10^{-5}eV^2$ (as well as $\sin^2\theta_{12}=0.304$) one can calculate a scaling factor which in turn can be expressed as -5.1±3.4% (day/night asymmetry of the

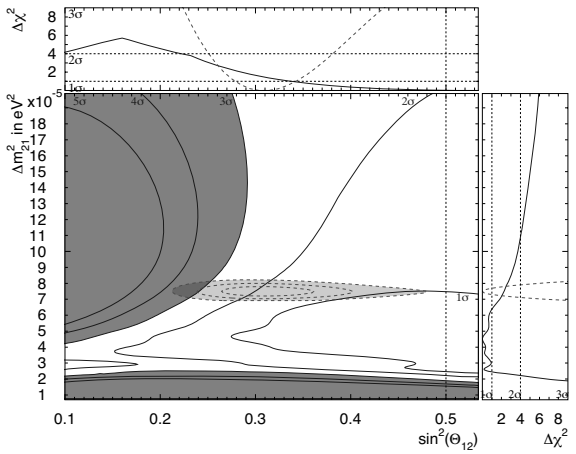

Fig. 6. Solar neutrino oscillation parameter regions excluded by Super-Kamiokande spectral and day/night data at 1, 2, 3, 4, and 5σ confidence levels (solid lines). Overlaid (dashed lines) are the allowed regions from KamLAND data at 1, 2, and 3σ confidence levels.

survival probability at 10 MeV). Similarly, the SNO measurement can be converted to an SK-I day/night asymmetry value of -2.9±1.9%. In this way, SK and SNO measure the day/night survival probability asymmetry at 10 MeV as -5.1±1.8%, or the SK-I day/night asymmetry as -2.9±1.0%. This combined result differs from zero by 2.9σ. The expected day/night asymmetry for these oscillation parameters is -5.69% (10 MeV day/night asymmetry) or -3.22% (SK-I day/night asymmetry).

6. Oscillation Analysis

We analysed the SK-IV elastic scattering rate, the recoil electron spectral shape, and the day/night variation to constrain the solar neutrino oscillation parameters. We then combined the SK-IV constraints with those of previous SK phases as well as other solar neutrino experiments. The measured elastic scattering rates $d_b^p \pm \sigma_b^p$ in energy bin b and phase p are fit to calculations b_b^p (from ^{8}B neutrinos, scaled by flux parameter β) and h_b^p (from hep neutrinos, scaled by flux parameter η). The spectrum+rate χ^2 of SK phase p is then

$$\chi_p^2 = \sum_{b=1}^{N_b}\left(\frac{d_b^p - f_p\left(\nu,\varepsilon_p,\rho_p\right)\times\left(\beta b_b^p\left(\sin^2\theta_{12},\Delta m_{21}^2\right)+\eta h_b^p\right)}{\sigma_b^p}\right)^2$$

$$= \chi_{p,\min}^2 + \begin{pmatrix} \beta-\beta_{\min}^p & \eta-\eta_{\min}^p \end{pmatrix}\cdot C_p \cdot \begin{pmatrix} \beta-\beta_{\min}^p \\ \eta-\eta_{\min}^p \end{pmatrix}$$

where f_p is the spectral distortion due to the neutrino spectrum uncertainty, energy scale, and energy resolution uncertainty described by the nuisance parameters ν, ε_p, and ρ_p. We assume a fixed value for θ_{13}: $\sin^2\theta_{13}$=0.025 (based on [7]). The minimum, the best-fit neutrino fluxes, and a 2×2 curvature matrix C_p uniquely describe the χ^2 of phase p. Before combining the phases, we scale the curvature matrix to account for the additional systematic uncertainty of the total rate (integrated over all energies; for SK-III and IV see Table 1 and 2) which is not covered by σ_b^p:

$$\chi^2 = \underset{\nu,\varepsilon_p,\rho_p,\beta,\eta}{\mathrm{Min}}\left[\nu^2+\left(\frac{\beta-\beta_0}{\sigma_\beta}\right)^2+\left(\frac{\eta-\eta_0}{\sigma_\eta}\right)^2+\right.$$

$$\left.\sum_{p=1}^{4}\left(\chi_{p,\min}^2+\frac{\sigma_{p,\mathrm{stat}}^2}{\sigma_{p,\mathrm{stat}}^2+\sigma_{p,\mathrm{syst}}^2}\begin{pmatrix} \beta-\beta_{\min}^p & \eta-\eta_{\min}^p \end{pmatrix}\cdot C_p\cdot\begin{pmatrix} \beta-\beta_{\min}^p \\ \eta-\eta_{\min}^p \end{pmatrix}+\varepsilon_p^2+\rho_p^2\right)\right]$$

Initially, we leave out the constraining terms for the neutrino flux parameters β (second term) and η (third term). The day/night variation data of each SK phase is represented by a log(likelihood) difference between the case of a day/night variation as predicted by the oscillation parameters, and a constant interaction rate (see [5] for details). The log(likelihood) differences of all SK phases are added, multiplied by -2, and added to the spectral (and total rate) χ^2. Figure 6 shows the resulting excluded areas of solar neutrino oscillation parameters. In the right panel of Figure 6 there is a slight tension between this and KamLAND's measurement of the solar Δm^2 (unlike Figure 5). Even though the expected amplitude agrees well within 1σ with the fitted amplitude for any Δm^2 in either the KamLAND or the SK range, the SK data somewhat favor the shape of the variation predicted by values of Δm^2 that are smaller than KamLAND's.

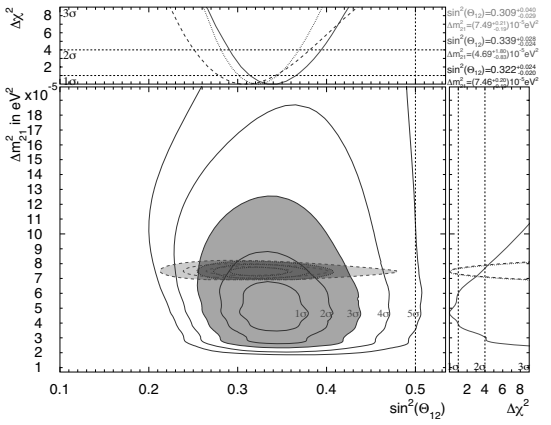

Fig. 7. Solar neutrino oscillation parameter regions allowed by Super-Kamiokande rate, spectral and day/night data at 1, 2, 3, 4, and 5σ confidence levels (solid lines). Overlaid (dashed lines) are the allowed regions from KamLAND data at 1, 2, and 3σ confidence levels and a combined fit (dotted lines).

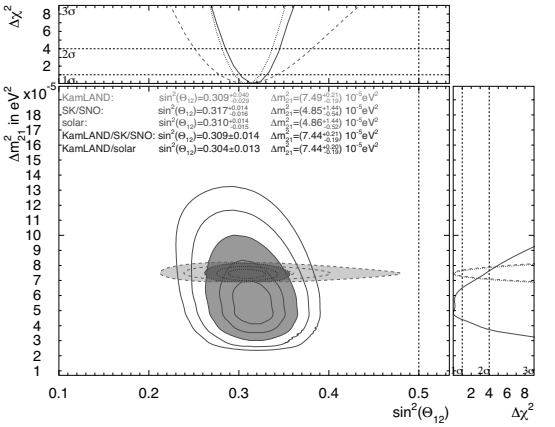

Fig. 8. Solar neutrino oscillation parameter regions allowed by Super-Kamiokande rate, spectral and day/night data and SNO rates, spectral and day/night data at 1, 2, 3, 4, and 5σ confidence levels (solid lines). Overlaid (dashed lines) are the allowed regions from KamLAND data at 1, 2, and 3σ confidence levels and a combined fit (dotted lines).

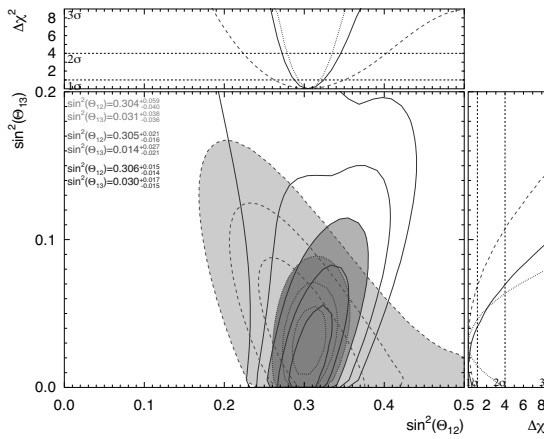

Fig. 9. Three flavor allowed regions from solar (dark gray) and KamLAND (light gray, dashed lines) data at 1, 2, and 3σ confidence levels. The combined fit (dotted lines) is in good agreement with recent measurements of θ_{13}.

If the ^{8}B flux in the fit to all SK data is constrained to $(5.25\pm0.20)\times10^6/(\mathrm{cm}^2\mathrm{sec})$ (motivated by [6]), the allowed areas of Figure 7 result. In that case SK measures the solar neutrino oscillation parameters to $\sin^2\theta_{12} = 0.339^{+0.028}_{-0.024}$ and $\Delta m^2_{21} = 4.69^{+1.80}_{-0.83}\times10^{-5}\mathrm{eV}^2$. The tension between KamLAND and SK's measurement of Δm^2 is slightly stronger in the ^{8}B flux constrained fit.

It is relatively straightforward to combine the SK solar neutrino oscillation constraints with SNO's [6], since the SNO χ^2 is of the same form as that of an SK phase. In that case, the hep neutrino flux must be constrained to $(7.88\pm1.26)\times10^3/(\mathrm{cm}^2\mathrm{sec})$, since SNO subtracts a fixed hep neutrino contribution and fits the ^{8}B flux afterwards. Figure 8 shows the allowed areas. The oscillation parameters are determined to be $\sin^2\theta_{12} = 0.317^{+0.014}_{-0.016}$ and $\Delta m^2_{21} = 4.85^{+1.44}_{-0.54}\times10^{-5}\mathrm{eV}^2$. We also perform a global fit to all solar neutrino measurements; this affects the allowed regions only marginally: the parameters of the global solar fit are $\sin^2\theta_{12} = 0.310^{+0.014}_{-0.015}$ and $\Delta m^2_{21} = 4.86^{+1.44}_{-0.52}\times10^{-5}\mathrm{eV}^2$. Adding KamLAND data [3] to this fit yields almost the same mixing ($\sin^2\theta_{13}$=0.304±0.013), but Δm^2 changes to $\Delta m^2_{21} = 7.44^{+0.20}_{-0.19}\times10^{-5}\mathrm{eV}^2$.

A three flavour fit to all solar neutrino and KamLAND data determines $\sin^2\theta_{13} = 0.030^{+0.017}_{-0.015}$ in good agreement with other measurements [7]. The θ_{12} mixing changes marginally ($\sin^2\theta_{12} = 0.306^{+0.015}_{-0.014}$) and the Δm^2 is unchanged. Figure 9 shows the θ_{12}–θ_{13} areas allowed by just the solar experiments, by only KamLAND, and by the global fit to both. Unlike KamLAND, solar neutrino data by itself has some sensitivity separating the two mixing angles since the oscillations of the higher energy solar neutrinos is dominated by matter effects, while vacuum oscillations govern the lower energy solar neutrinos. The uncertainties of the solar+KamLAND fit in determining both mixing angles are much smaller than those of the solar combined fit, because the high energy solar neutrino measurements of SK and SNO (driven by matter oscillations) dominate the solar fit, so KamLAND's vacuum-oscillating reactor anti-neutrinos produce a θ_{12}–θ_{13} anti-correlation while the solar data θ_{12}–θ_{13} correlation is positive.

7. Conclusions

Super-Kamiokande-IV measured the ^{8}B solar neutrino-electron elastic scattering rate, the recoil electron spectrum, and the solar zenith angle variation of the rate during 1069 live days, so far. The statistical precision is similar to that of the first phase, but systematic uncertainties are reduced, and the energy threshold is one MeV lower. The Super-Kamiokande solar neutrino data dominates the solar Δm^2 determination in the global solar neutrino oscillation fit. There is slight tension between Super-Kamiokande's value of Δm^2 and the reactor anti-neutrino measurement of KamLAND. Super-Kamiokande sees a slight hint of a non-zero day/night amplitude with a statistical significance of 2.3σ. Combined with SNO's measurement of the day/night asymmetry, the presence of an Earth matter effect is favored by 2.9σ. Super-Kamiokande has searched for the transition between vacuum dominated oscillations (lower energy solar neutrinos) and matter dominated oscillations (higher energy solar neutrinos) leading to a distortion of the recoil electron spectrum. There is no evidence of such a distortion. The predicted distorted spectrum is disfavored by 1.1 to 1.9σ compared to an undistorted spectrum.

References

[1] K. Abe et al, Phys. Rev. D83 052010 (2011).
[2] J. Hosaka et al, Phys. Rev. D73 112001 (2006).
[3] A. Gando et al, Phys Rev. D83 052002 (2011).
[4] A. Friedland, C. Lunardini, C. Peña-Garay, Phys. Lett. B594 347 (2004).
[5] M. Smy et al, Phys. Rev. D69 011104 (2004).
[6] B. Aharmim et al., arXiv:1109.0763, submitted to PRC.
[7] K. Abe et al, Phys. Rev. Lett. 107 041801 (2011); F. An et al, Phys. Rev. Lett. 108 171803 (2012); Phys. Rev. Lett. 108 191802 (2012).